The Nucleus **47**, No. 2 (2010) 131-135

**The Nucleus**
A Quarterly Scientific Journal of Pakistan
Atomic Energy Commission
NCLEAM, ISSN 0029-5698

# THERMAL PROPERTIES AND ACTIVATION ENERGY OF THE $[Zr_{0.645}Ni_{0.155}Al_{0.115}Cu_{0.085}]_{98}Si_2$ AMORPHOUS ALLOY

*M. IQBAL, J.I. AKHTER and Z.Q. HU[1]

Physics Division, Directorate of Science, PINSTECH, P.O. Nilore, Islamabad, Pakistan

[1]Institute of Metal Research (IMR), Chinese Academy of Sciences (CAS), 72 Wenhua Road, Shenyang 110016, P.R. China

(Received February 24, 2010 and accepted in revised form May 13, 2010)

Zr-based amorphous alloys are novel materials having wide range of applications. Melt spun amorphous ribbon with composition $(Zr_{0.645}Ni_{0.155}Al_{0.115}Cu_{0.085})_{98}Si_2$ of 50 μm thickness was synthesized to investigate the thermal properties and activation energy. Differential scanning calorimetry (DSC) was used to investigate these properties. X-ray diffraction (XRD) and scanning electron microscopy (SEM) were employed for phase analysis and microstructural study. Thermal parameters were derived from DSC measurements. Phases like $NiZr_2$, $CuZr_2$ and $SiZr_2$ were identified in the samples annealed at various temperatures. It was found that Si addition had positive effect on most of the thermal parameters.

**Keywords:** Amorphous alloys, Metallic glasses, Thermal properties, Crystallization, SEM, DSC

## 1. Introduction

Amorphous alloys have emerged as an excellent class of materials with combination of unique physical, chemical and thermal properties and have found wide range of applications [1-6]. There has been considerable research work on the amorphous alloys during the last two decades. Among the amorphous alloys, the Zr-Cu-Al-Ni alloys have been widely studied [1-3,7-9]. Many additional elements like Fe, Er, Nb, Ti, Ta, Y, Si, B, Be, C, Sc, W, Mo and Cr have been added in Zr-based alloys [2,7-18] to improve the thermal properties of amorphous alloys. Critical cooling rate for glass formation, glass-forming ability (GFA), crystallization behavior and thermal properties of amorphous materials have been found very sensitive to elemental addition [11]. A few reports are available which indicate that Si addition can enhance the activation energy [2,10,12]. Jang et al. [10] studied the crystallization behavior of Zr-Cu-Ni-Al by replacing Zr with Si and reported increase in activation energy. But most of the melt spun ribbons of Zr-based alloys having Si ≥ 2 at. % were found to be partially crystalline containing silicides. There is no report available containing results on thermal parameters like γ, δ, β and ω for alloys containing Si. Iqbal et al. [3] explored thermal properties of the bulk amorphous $Zr_{64.5}Ni_{15.5}Al_{11.5}Cu_{8.5}$ base alloy. The aim of the present study was to investigate the effect of Si addition on thermal properties and activation energy of $(Zr_{0.645}Ni_{0.155}Al_{0.115}Cu_{0.085})_{98}Si_2$ amorphous alloy. The Si addition affects the properties and glass-forming ability (GFA) of many systems like Fe, Zr, Mg and Cu-based amorphous alloys. Si atom is small in size (0.11530 nm) and can easily adjust itself in between the vacant spaces of other bigger atoms. On the other hand, Si addition can affect the melting and liquid temperatures of the base alloy. It is expected that Si addition would be beneficial for improving the thermal properties and thermal stability of the $Zr_{64.5}Ni_{15.5}Al_{11.5}Cu_{8.5}$ base alloy.

## 2. Experimental

The constituent metals Zr, Cu, Al, Ni and Si having 2-3 N purity, were washed and cleaned ultrasonically in ethanol. The precisely weighed mixture of the alloy constituents was melted in an arc melting furnace under Ti gettered atmosphere of high purity Ar at a pressure of about $4.5 \times 10^{-4}$ Pa. The alloy buttons having composition

* Corresponding author : miqbalchishti@yahoo.com

$(Zr_{0.645}Ni_{0.155}Al_{0.115}Cu_{0.085})_{98}Si_2$ were melted at least four times to get the extended chemical homogeneity. The composition was checked by energy dispersive spectroscopy (EDS) attached with the scanning electron microscope (SEM) which was used to examine the samples for microstructural studies. Error in the EDS analysis may be at least ± 2 % of the reported value. Synthesis of melt spun ribbon of 50 μm thickness and 3 mm width was carried out at vacuum approximately $1x10^{-3}$ Pa using single roller melt spinning technique. Bulk amorphous ingots of 1-3 mm thickness were also tried to synthesize by Cu mold casting technique at pressure of approximately $1x10^{-3}$ Pa. For thermal analysis, differential scanning calorimetry (DSC) measurements were conducted using NETZSCH DSC 404 C at heating rates "r" of 10, 20 and 40 K/min under Ar atmosphere. For structural characterizations X-ray diffraction (XRD) was conducted using Rigaku D/Max-2500 X-ray diffractometer with Cu $K\alpha_1$ (1.54056 Å) radiation. In order to study crystallization behavior and nature of phases, the alloy samples were annealed in the box type furnace at 673 K, 713 K and 825 K for 20 minutes each encapsulating in quartz capsules under high purity Ar atmosphere to avoid oxidation.

## 3. Results and Discussion

The compositions of a number of pieces of melt spun ribbon were checked by EDS. The average composition was found to be close to the designed composition within the experimental error limits. The XRD patterns of the as-cast and annealed samples of the alloy are shown in Fig. 1 (a-d). A broad band for the as-cast sample shown in Fig. 1(a) indicates the amorphous nature of the alloy. It is due to disorder atomic structure. The precipitates are analyzed and found to be binary

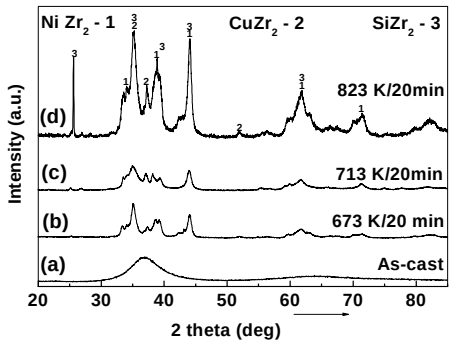


Figure 1 (a-d). XRD patterns of the as-cast (a) and annealed samples of the alloy (b-d).

type. Zirconium content is the maximum in all the phases. EDS results show that precipitates are rich in Si, Ni and Cu. The phases identified in the annealed samples are $NiZr_2$ and $CuZr_2$ and $SiZr_2$ designated as 1, 2 and 3 respectively as shown in Fig. 1(b-d). Results show that $SiZr_2$ phase starts to nucleate at 673 K while $NiZr_2$ and $CuZr_2$ phases start to appear at higher temperature. The $SiZr_2$ is the major phase at 823 K. Atomic radii [19] and heats of mixings ($\Delta H_{mix}$) [20] of the alloy constituents are given in Table 1. The first phase nucleated is $SiZr_2$. The reason is the lowest atomic size of Si (0.1153 nm) atom and the highest negative heat of mixing of Zr-Si pair (-84 kJ/mol). The second phase nucleated after $SiZr_2$ is $NiZr_2$. The reason is that Ni is a solute having the highest concentration (15.5 at. %) in the alloy. It has slightly larger atomic radius (0.12459 nm) than Si. The negative heat of mixing of Ni-Zr pair is lower (-49 kJ/mol) than Zr-Si pair. The third phase nucleated is $CuZr_2$. Physical appearance of the melt spun ribbon revealed excellent metallic glassy luster with mirror like finishing that also indicates the amorphous structure. SEM examination of the as-cast ribbon revealed featureless surface as shown

Table 1. Mixing enthalpies and atomic radii of alloy constituents

| Element | Atomic radii (nm) | Mixing enthalpies ($kJmol^{-1}$) | | | | |
|---|---|---|---|---|---|---|
| | | Zr | Al | Ni | Cu | Si |
| | | 0.16025 | 0.14317 | 0.12459 | 0.12780 | 0.11530 |
| Zr | 0.16025 | - | -44 | -49 | -23 | -84 |
| Al | 0.14317 | -44 | - | -22 | -1 | -19 |
| Ni | 0.12459 | -49 | -22 | - | 4 | -40 |
| Cu | 0.12780 | -23 | -1 | 4 | - | -19 |
| Si | 0.11530 | -84 | -19 | -40 | -19 | - |

in Fig. 2. It reconfirmed the amorphous structure of the alloy. Bulk ingots of thickness ≥ 1 mm show crystalline structure with dull appearance. Fig. 3 shows secondary electron image (SEI) of 3 mm bulk sample. Formation of zirconium silicide is clear which nucleated due to low cooling rate during Cu mold casting by using induction furnace. Therefore, melt spun amorphous ribbon of 50 μm thickness was successfully synthesized by melt spinning technique.


Figure 2. Featureless surface of 50 μm thick as-cast melt spun ribbon.

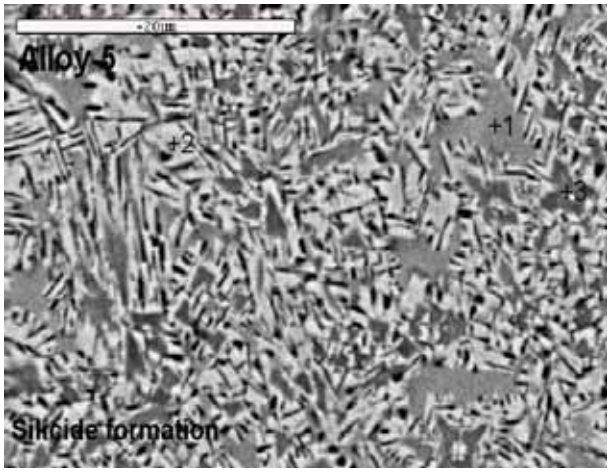


Figure 3. Precipitation in 3 mm thick bulk ingot of the alloy. Phases are marked.

Fig. 4 shows DSC plots of the alloy studied at heating rate "r" of 10, 20 and 40 K/min. DSC plots show an endothermic reaction characteristic of the glass transition, followed by a large supercooled liquid region and then an exothermic peak corresponding to the crystallization. At high temperature, the two endothermic peaks correspond to the melting and liquid transitions. The alloy shows single stage crystallization at all heating rates "r". Different thermal parameters such as glass transition temperature $T_g$, peak temperature $T_p$, supercooled liquid region $\Delta T_x = T_x - T_g$, where $T_x$ is crystallization temperature, a key parameter usually called reduced glass transition temperature $T_{rg1} = T_g/T_m$ and $T_{rg2} = T_g/T_l$ [2,18,21], $\gamma$ parameter = $T_x/(T_l+T_g)$ [2,18], $\delta$ parameter = $T_x/(T_l-T_g)$ [22], parameter $\beta = T_g * T_x/(T_l-T_x)^2$ [23] and

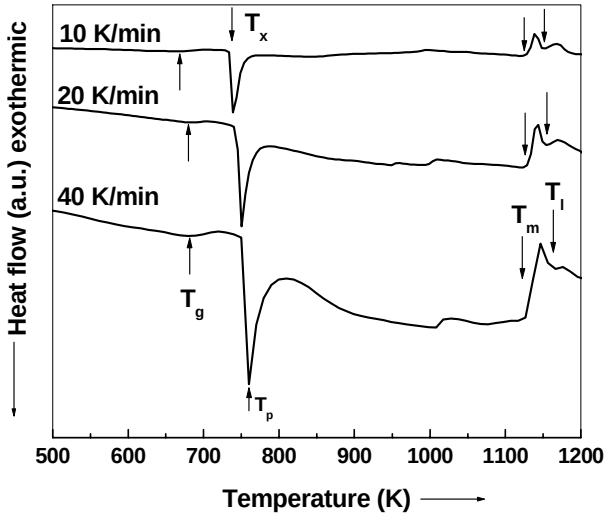


Figure 4. DSC scans of the alloy studied at different heating rates.

parameter $\omega = T_g/T_x - 2T_g/(T_g+T_l)$ [24] were calculated and are given in Table 2. Si addition in the base alloy shows positive effect on key parameter $T_{rg}$, $\delta$, $\beta$ and $\omega$ parameters [3]. The value of $\Delta T_x$ was found to be 68 ± 2 K for the alloy which is higher than the alloys studied by Jang et al. [10] and Qi et al. [14]. The values of the thermal parameters $T_{rg1}$, $T_{rg2}$, $\delta$, $\beta$ and $\omega$ enhanced considerably by Si addition in the base alloy. It is clear that most of the thermal parameters of the $[Zr_{0.645}Ni_{0.155}Al_{0.115}Cu_{0.085}]_{98}Si_2$ alloy are better than the base alloy as given in Table 2. It means that Si addition is beneficial for enhancement of thermal properties which is due to small atomic size of Si as discussed before.

The activation energy ($E_{ac}$) for crystallization of an alloy is an important kinetic parameter. Activation energy ($E_{ac}$) for crystallization was calculated using the Kissinger [25] equation ($\ln(r/T_p^2) = (-E_{ac}/RT_p)$ + constant) and Ozawa equation $\ln(r) = -E_{ac}/T_p$ + constant, here, $T_p$ represents the peak temperature, r is the heating

Table 2. Comparison of thermal parameters of the base alloy $Zr_{64.5}Ni_{15.5}Al_{11.5}Cu_{8.5}$ and $[Zr_{0.645}Ni_{0.155}Al_{0.115}Cu_{0.085}]_{98}Si_2$ alloy at different heating rates (All temperatures are in K).

| Alloy | r | $T_g$ | $T_p$ | $T_m$ | $T_l$ | $T_g/T_m$ | $T_g/T_l$ | $\gamma$ | $\delta$ | $\beta$ | $\omega$ |
|---|---|---|---|---|---|---|---|---|---|---|---|
| Base alloy | 10 | 635 | 739 | 1103 | 1129 | 0.576 | 0.563 | 0.41 | 1.469 | 2.83 | 0.156 |
| | 20 | 640 | 740 | 1098 | 1128 | 0.583 | 0.568 | 0.41 | 1.508 | 3.05 | 0.147 |
| | 40 | 649 | 760 | 1107 | 1137 | 0.586 | 0.571 | 0.42 | 1.535 | 3.24 | 0.138 |
| Present alloy Si = 2 % | 10 | 669 | 739 | 1123 | 1149 | 0.596 | 0.573 | 0.41 | 1.53 | 2.89 | 0.173 |
| | 20 | 680 | 751 | 1125 | 1149 | 0.604 | 0.592 | 0.41 | 1.59 | 3.12 | 0.166 |
| | 40 | 682 | 760 | 1127 | 1155 | 0.605 | 0.591 | 0.41 | 1.59 | 3.16 | 0.164 |

rate and R is the real gas constant having value 8.3145 J/mol-K with slope $-E_{ac}/R = B$, where B is a constant. Data on heating rate "r" and peak temperature $T_p$ was plotted as shown in Fig. 5 in terms of $1000/T_p$ versus $\ln(r/T_p^2)$ for Kissinger and

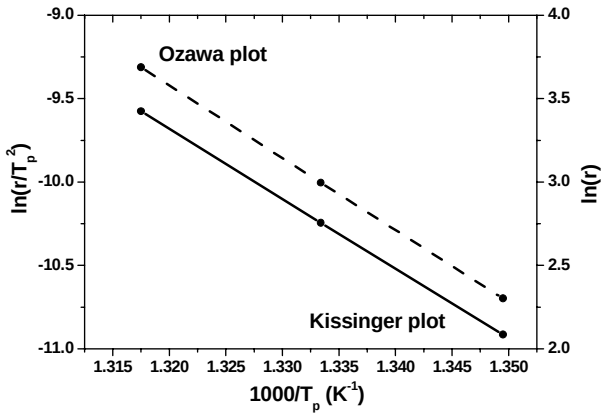


Figure 5. Kissinger and Ozawa plots for calculation of activation energy.

$1000/T_p$ versus ln(r) for Ozawa equations, respectively. The value of the slope B was measured from the plots. Putting the values of R and B, activation energies for the first stage crystallization were calculated. The activation energy was found to be 348 and 360 kJ/mol for the present alloy by Kissinger and Ozawa equations respectively. On the other hand base alloy have the activation energy of 268 and 303 kJ/mol by Kissinger and Ozawa plots respectively. The activation energy of the alloy was found to be comparable with the alloys reported by Jang et al. [10] and approximately 30 % higher than the activation energy of the base alloy using Kissinger equation and 19 % by Ozawa equation. The enhancement in activation energy is due to improved thermal parameters by Si addition. The higher activation energy of the present alloy as compared to the base alloy indicates good thermal stability of the alloy.

## 4. Conclusions

Melt spun amorphous ribbon having composition $(Zr_{0.645}Ni_{0.155}Al_{0.115}Cu_{0.085})_{98}Si_2$ of 50 μm thickness was produced by single roller melt spinning technique. The alloy showed enhancement in reduced glass transition temperature $T_{rg}$, $\delta$, $\beta$ and $\omega$ thermal parameters due to Si addition in the base $Zr_{64.5}Ni_{15.5}Al_{11.5}Cu_{8.5}$ alloy. The activation energy of crystallization for the present alloy was found to be 30 % and 19 % higher than the base alloy by Kissinger and Ozawa equations respectively. Present alloy shows good thermal stability and Si addition has positive effect on most of the thermal properties. Phases like $SiZr_2$, $NiZr_2$ and $CuZr_2$ were identified in the annealed samples.

## Acknowledgements

The authors gratefully acknowledge the technical support provided by Prof. H.F. Zhang, IMR, CAS, Shenyang, P.R. China, Dr. Maqsood Ahmad as well as all members of MSG and Diagnostic Lab. Physics Division, PINSTECH, Islamabad.

## References

[1] M. Telford, Mater. Today **7** (2004) 36.

[2] C.T. Liu and Z.P. Lu, Intermetallics **13** (2005) 415.

[3] M. Iqbal, J.I. Akhter, W.S. Sun, H.F. Zhang and Z.Q. Hu, J. Alloy Compd. **422** (2006) 218.

[4] A.R. Yavari and J.J. Lewandowski and J. Eckert, Mater. Res. Bull. **32** (2007) 635.

[5] N. Nishiyama, K. Amiya and A. Inoue, J. Non-Cryst. Solids **353** (2007) 3615.

[6] A. Inoue and N. Nishiyama. Mater. Res. Bull. **32** (2007) 651.

[7] M. Iqbal, Z.Q. Hu, H.F. Zhang, W.S. Sun and J.I Akhter, J. Non-Cryst. Solids **352** (2007) 3290.

[8] M. Iqbal, J.I. Akhter, W.S. Sun, J.Z. Zhao, M. Ahmad, W. Wei, Z.Q. Hu and H.F. Zhang, Mater. Lett. **60** (2006) 662.

[9] M. Iqbal, W.S. Sun, H.F. Zhang, J.I. Akhter and Z.Q. Hu. Mater. Sci. Eng. A. **447** (2007) 167.

[10] J.S.C. Jang, Y.W. Chen, L.J. Chang, H.Z. Cheng, C.C. Huang and C.Y. Tsau, Mater. Chem. Phys. **89** (2005) 122.

[11] Q. Wang, J. M. Pelletier, Y. D. Dong and Y.F. Ji, Mater. Sci. Eng., A **370** (2004) 316.

[12] W.H. Wang, Z.B. Bian, P. Wen, Y. Zhang, M.X. Pan and D.Q. Zhao, Intermetallics **10** (2002) 1249.

[13] M. Iqbal, J.I Akhter, H.F. Zhang and Z.Q. Hu. J. Non-Cryst. Solids **354** (2008) 3291.

[14] M. Qi, X.D. Wang, S. Deledda, J. Eckert and L. Schultz, J. Mater. Sci. Lett. **21** (2002) 893.

[15] J.G. Wang, B. W. Choi, T. G. Nieh and C. T. Liu, J. Mater. Res. **15** (2000) 798.

[16] K.Q. Qiu, A. M. Wang, H. F. Zhang, B. Z. Ding and Z. Q. Hu, Intermetallics **10** (2002) 1283.

[17] Y.F. Sun, T.L. Cheung, Y.R. Wang, C.H. Shek, W.H. Li and B.C. Wei, Mater. Sci. Eng. A **398** (2005) 22.

[18] Z.P. Lu, H. Bei and C.T. Liu, Intermetallics, **15** (2007) 618.

[19] O.N. Senkov and D.B. Miracle, Mater. Res. Bull. **36** (2001) 2183.

[20] A. Takeuchi and A. Inoue, Mater. Trans. **46** (2005) 2817.

[21] Y. Li. J. Mater. Sci. Technol. **15** (1999) 97.

[22] Q.J. Chen, J. Shen, D. Zhang, H. Fan, J. Sun and D.G. McCartney, Mater. Sci. Eng. A **433** (2006) 155.

[23] Z.Z. Yuan, S.L. Bao, Y. Lu, D.P. Zhang and L.Yao. J. Alloy. Compd. **459** (2008) 251.

[24] Z.L. Long, H.Q. Wei, Y.H. Ding, P. Zhang, G.Q. Xie and A. Inoue, J. Alloy. Compd. **475** (2009) 207.

[25] H.E. Kissinger, Anal. Chem. **29** (1957) 1702.